Detection of a directly modulated terahertz light with quantum-well photodetector

Qingzhao Wu (武庆钊), Li Gu (顾 立), Zhiyong Tan (谭智勇), Chang Wang (王 长), and Juncheng Cao (曹俊诚)*

Key Laboratory of Terahertz Solid-State Technology, Shanghai Institute of Microsystem and Information Technology, Chinese Academy of Sciences, Shanghai 200050, China

**Corresponding author: jccao@mail.sim.ac.cn*

Received July 28, 2014; accepted October 11, 2014; posted online December 3, 2014

We demonstrate a wireless transmission link at 3.9 THz over a distance of 0.5 m by employing a terahertz (Hz) quantum-cascade laser (QCL) and a THz quantum-well photodetector (QWP). We make direct voltage modulation of the THz QCL and use a spectral-matched THz QWP to detect the modulated THz light from the laser. The small signal model and a direct voltage modulation scheme of the laser are presented. A square wave up to 30 MHz is added to the laser and detected by the THz detector. The bandwidth limit of the wireless link is also discussed.

OCIS codes: 140.5965, 040.2235, 060.2605.
doi: 10.3788/COL201412.120401.

Terahertz (THz) technology has attracted more and more attention in the past two decades because of its various kinds of potential applications, such as real-time imaging, information, and short range wireless communication among others[1–4]. For these applications, THz emitter and receiver are two key components. There are several different THz emitters, including uni-traveling carrier photodiode[5], resonant tunneling diode[6], and microwave multiplication[7], which mostly operate in the sub-THz region from 100 to 300 GHz. However, there are not any devices mature enough to build a high-speed THz communication system in the range of 2.0–5.0 THz yet. Owing to the obvious advantages such as high emitting power, fast response, THz quantum-cascade laser (QCL) is a very promising emitter of THz wave especially above 1 THz frequency[8,9]. The study of high-speed modulation of the THz QCL is important for the application of the device. Since the lifetime of the internal transport carrier in the THz QCL is very short, the direct modulation of device can reach the frequency of tens of gigahertzs[10,11]. On the other hand, the THz quantum-well photodetector (QWP)[12,13] is a good choice as a receiver. THz QWP has some specific characteristics, including high response speed, high sensitivity, and narrow band response, which is potentially suitable for detecting THz light. A wireless communication demonstration with a THz QCL and THz QWP was first reported by Grant *et al.* at 3.8 THz in 2009[14], which shows the basic components needed for a wireless communication can be performed by using a THz QCL as a source and a THz QWP as a receiver. Till date, there are a few reports about THz wireless communication based on THz QCL and THz QWP[15,16].

In this letter, firstly, we present a direct voltage modulation scheme of the THz QCL by employing a square wave signal. A spectral-matched THz QWP is used to detect the output THz light from the source. Secondly, the direct modulation and the small signal model of the THz QCL as well as the bandwidth limit of the wireless link are analyzed.

The THz QCL is based on a GaAs/AlGaAs material system with a four-well resonant phonon structure of the active region, as well as a metal-metal waveguide, emitting at 3.9 THz. The active region of the device has a size of 15 mm×25 μm and a height of 10 μm. The output power of the laser is around 2 mW in the continuous-wave mode. In order to achieve the best performance of the devices, the THz QCL is placed on a copper heat sink and mounted on the cold finger of a closed cycle helium cryostat, operating at 10 K, and the THz QWP is cooled down to 4 K by using a continuous-flow liquid-helium cryostat.

A schematic experimental setup is shown in Fig. 1. The THz QCL is driven by a modulator. The modulator module mainly includes a high-speed amplifier, which has a magnification of $A = V_o/V_{IN} = (R_G + R_F)/R_G$. By using a bias-T, the direct current (DC) bias is added to the alternate current (AC) component. In this experiment, the DC bias added to the laser is 12.55 V and the AC bias is 0.45 V. The high voltage is in the linear operation range of the laser and at the same time, the low voltage is below the threshold voltage of the laser. The modulation depth of the signal is 100%, and the modulation is on-off keying.

Two off-axis parabolic mirrors are used between the laser and the detector to establish a 0.5 m optical path in the room air. The emitting THz light is collected by the two off-axis parabolic mirrors with a focal length of 101.6 mm, and then focused onto the detector through the polyethylene window of the closed cycle cryostat where the detector is placed. The transmission of the

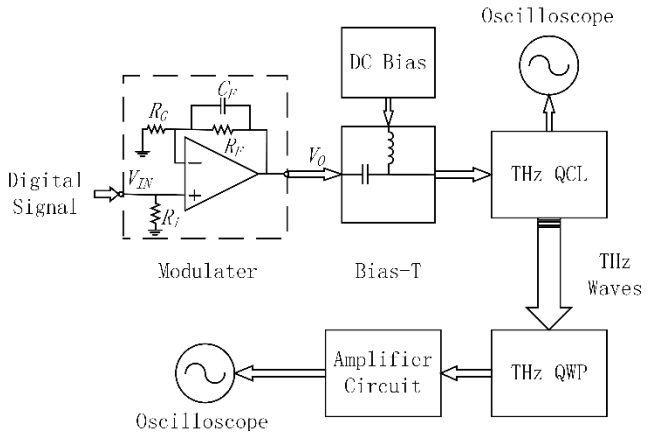

Fig. 1. Scheme of the transmission setup.

polyethylene window is 75% at 3.9 THz with 1.8 mm thickness. At 3.21 THz the peak responsivity is 0.5 A/W and the detectivity is about 10^{11} cmHz$^{1/2}$/W[17]. The responsivity and detectivity fall to 55% of the peak at the frequency of 3.9 THz. The bias voltage added to the THz QWP is −50 mV, provided by a transimpedance amplifier (TIA) circuit. The photocurrent from the detector is converted to voltage by the TIA and amplified by a variable gain amplifier, and is then shown in the oscilloscope.

The power–voltage–current (*P-V-I*) curve of the THz QCL is shown in Fig. 2. It is clear that the threshold current is about 0.15 A. The linearity of the *P-V-I* curve of the device is relatively better in the range of 0.16 to 0.19 A and within this range the voltage is from 12.7 to 13.5 V. We can take advantage of this feature to make direct voltage modulation of the laser. A spectral-matched THz QWP is used to detect the THz light from the laser. By using a spectroscope, we can get the normalized spectra of the laser emission and the detector response (Fig. 3). It is clear that the

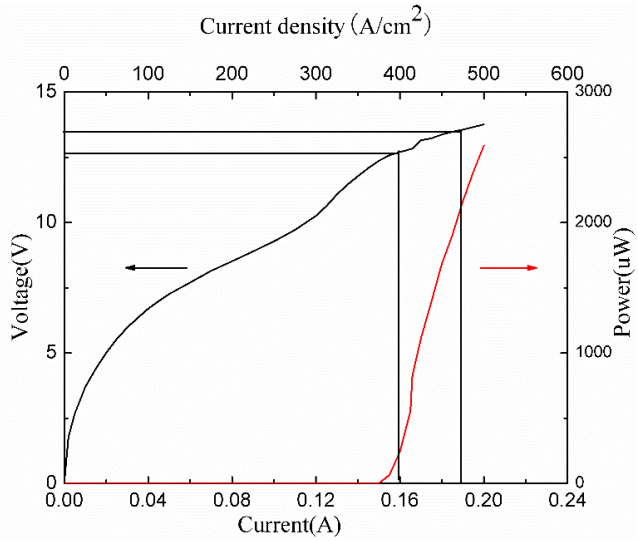

Fig. 2. *P-V-I* curve of the THz QCL.

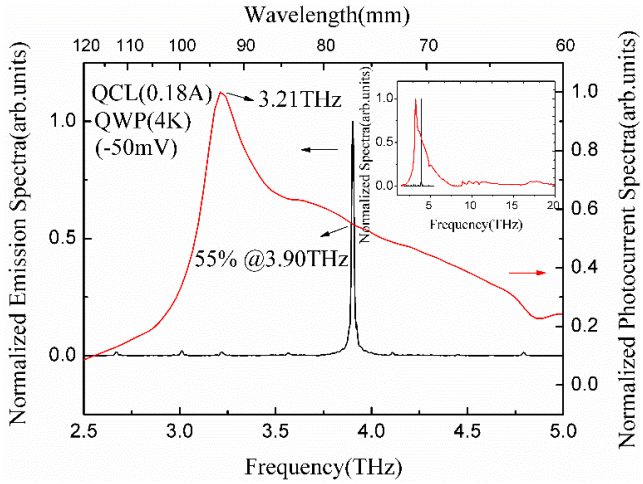

Fig. 3. Normalized spectra of the THz laser emission and the detector response. The inset is the illustration of a wider frequency range.

THz QCL emission spectrum is very narrow and the frequency range corresponds to the relatively flat photocurrent spectra of the THz QWP. Therefore, using the THz QWP to detect the 3.9 THz light is reasonable and practical.

For small signals, the lumped electrical model of the THz QCL can be simplified as a device-differential resistance R_d in parallel with a small capacitor (Fig. 4). The resistance R_d can be calculated from derivation of the *P-V-I* curve in Fig. 2 at the bias voltage in operation range, that is $R_d = \Delta V/\Delta I$, which is about 20 Ω. Ignoring the influence of the top and the bottom contacts, the parallel capacitance C can be calculated by $C = \varepsilon_0\varepsilon_r A/h$, where ε_0 is the vacuum permittivity, ε_r is the relative permittivity of the material of the active region (GaAs/AlGaAs), A is the active region area, and h is the thickness of the active region. We can get the value of the capacitance by measurement, which is about 10 pF.

When the device is connected to a coaxial cable, the impedance R of the coaxial cable must be taken into consideration, and the inductance L is caused by the wire bond. Ignoring the parasitic inductance L and the bandwidth limit of the modulation circuit, we can get the theoretically calculated −3 dB bandwidth as

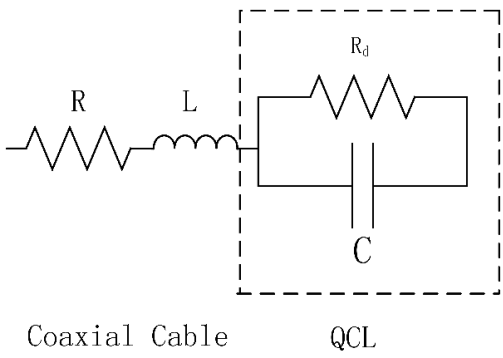

Fig. 4. Electrical model of small signal of the THz QCL.

$f_{-3\mathrm{dB}} = (R + R_\mathrm{d})/2\pi R R_\mathrm{d} C$. In our experiment, we obtain the $f_{-3\mathrm{dB}}$ as 1.11 GHz. The −3 dB bandwidth of the THz QCL is primarily affected by the differential resistance R_d and the capacitance of the parallel capacitor C.

A 10 MHz square wave signal from the digital signal generator is added to the THz QCL. The time traces of the modulation signal and the demodulation signal are shown in Fig. 5(a). The upper trace shows the modulation signal and the lower trace shows the demodulation signal. We then gradually increase the frequency of the input square wave signal to 30 MHz. The time traces of the modulation and demodulation signals are shown in Fig. 5(b).We can get received signal from the demodulation circuit, meaning that there is THz light in the optical path and the source is modulated correctly. The received signal can be correctly judged. Thus, the wireless link can be used in the transmission of digital signal.

Owing to the delay of the circuit and the response time of the device, the demodulation signal shows a delay of about 75 ns in Fig. 5(a) and a delay of about 25 ns in Fig. 5(b). A slight overshoot and undershoot can be found in Fig. 5(a), which can be suppressed by the adjustable capacitor C_F. Some nonlinear distortion of the modulation signal can be found in Fig. 5(b). It has been discussed that the $f_{-3\mathrm{dB}}$ of the small signal is 1.11 GHz, which is much higher than the frequency modulation. We attribute the distortion to the nonlinear and the bandwidth limit of the modulation circuit. Square wave signal is mathematically equivalent to the sum of a sine wave at the same frequency, plus an infinite series of odd-multiple frequency sine waves at diminishing amplitude and the higher odd-multiple harmonics are filtered out by the modulation circuit. The wavelength of 30 MHz signal is 10 m and the length of the coaxial cable connected to the laser is 1.5 m, which is comparable to the wavelength of the modulation signal. There is impedance mismatch between the coaxial cable and the laser, which leads to the reflection of the power. The superposition of the reflection signal and the original signal causes attenuation and distortion.

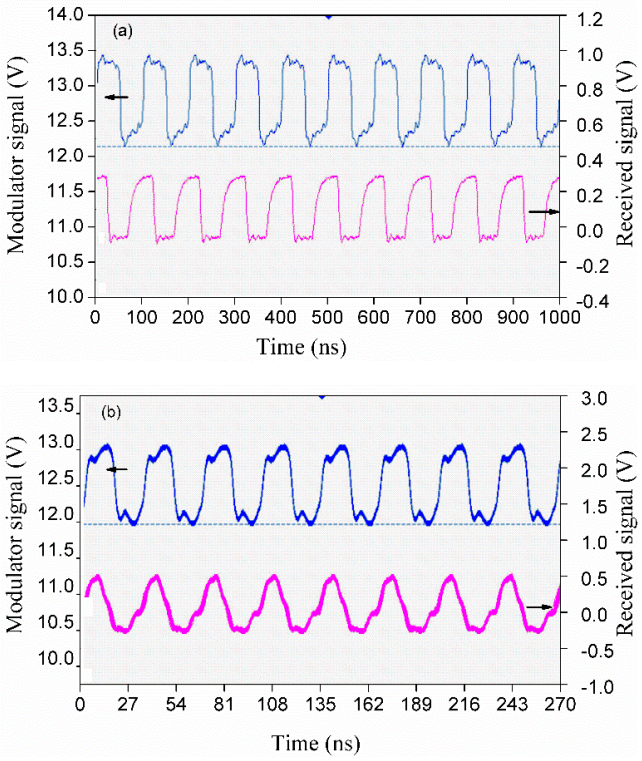

Fig. 5. Time trace of (a) 10 and (b) 30 MHz signal applied to emitter (upper trace) and received signal (lower trace).

For the received signal, besides the distortion caused by modulation signal, the bandwidth limit and noise of the home-made receiving circuit is another key factor. The receiving circuit module mainly includes a TIA and a variable gain amplifier. The bandwidth limit of the TIA is the main bandwidth limit of the demodulation circuit as well as the transmission link. We take advantage of a voltage feedback amplifier as a TIA to supply the bias voltage needed by the QWP and convert the photocurrent to a voltage signal[15]. The −3 dB bandwidth of the TIA is theoretically calculated as $f_{-3\mathrm{dB}} = \sqrt{\mathrm{GBP}/(2\pi C_\mathrm{T} R_\mathrm{F})}$, where GBP is the gain bandwidth product of the operational amplifier, which is 1.6 GHz. C_T is the total capacitance of the operational amplifier including the THz QWP capacitance and the parasitic input capacitance of the operational amplifier. In our experiment, we choose a transimpedance R_F of 1 kΩ, C_T is 380 pF, thus the $f_{-3\mathrm{dB}}$ is 25.9 MHz. When the frequency of the modulation signal is 30 MHz, it is higher than the $f_{-3\mathrm{dB}}$ of the TIA. The higher odd-multiple harmonics of the signal are attenuated greatly by the TIA circuit and only the baseband signal is retained, which makes the demodulation signal look like a sine signal. By reducing the capacitance of the detector and the transimpedance R_F, the −3 dB bandwidth of the TIA can be improved.

In conclusion, we present a direct voltage modulation scheme of THz QCL, as well as a wireless link over a distance of 0.5 m by employing a THz QWP to detect the THz light from the laser. The maximum transmission bandwidth is 30 MHz. The result shows that the THz light is modulated and detected correctly in the wireless link. We discuss the direct voltage modulation and the small signal model of the THz QCL as well as the bandwidth limit of the transmission link. In our experimental setup, constrained by the performance of the devices and digital circuits in the system, the bandwidth of the link cannot reach gigahertz. Nevertheless, the system shows the potential of wireless communication with THz QCL and THz QWP. By optimizing the devices and the circuits, the bandwidth of the transmission link is expected to improve significantly.

This work was supported by the National 973 Program of China (No. 2014CB339803), the National 863 Program of China (No. 2011AA010205), the National

Natural Science Foundation of China (Nos. 61131006, 61321492, 61176086, 61204135, and 61306066), the Major National Development Project of Scientific Instrument and Equipment (No. 2011YQ150021), the National Science and Technology Major Project (No. 2011ZX02707), the Major Project (No. YYYJ-1123-1), and the International Collaboration and Innovation Program on High Mobility Materials Engineering of the Chinese Academy of Sciences and the Shanghai Municipal Commission of Science and Technology (No. 13ZR1464600).

References

1. M. Tonouchi, Nat. Photon. **1,** 97 (2007).
2. Z. Tan, L. Gu, T. Xu, T. Zhou, and J. Cao, Chin. Opt. Lett. **12,** 070401 (2014).
3. T. Nagatsuma, H. Nishii, and T. Ikeo, Photon. Res. **2,** B64 (2014).
4. A. J. Seeds, in *Proceedings of Optical Fiber Communication* Th4H.1 (2014)
5. H. J. Song, K. Ajito, Y. Muramoto, A. Wakatsuki, T. Nagatsuma, and N. Kukutsu, Electron. Lett. **48,** 953 (2012).
6. M. Asada, S. Suzuki, and N. Kishimoto, Jpn. J. Appl. Phys. **47,** 4375 (2008).
7. C. Jastrow, K. Münter, R. Piesiewicz, T. Kürner, M. Koch, and T. Kleine-Ostmann, Electron. Lett. **44,** 213 (2008).
8. R. Köhler, A. Tresicucci, F. Beltram, H. E. Beere, E. H. Linfield, A. G. Davies, D. A. Ritchie, R. C. Iotti, and F. Rossi, Nature **417,** 156 (2002).
9. S. Kumar, IEEE J. Sel. Top. Quant. Electron. **17,** 38 (2011).
10. P. Gellie, S Barbieri, J. F. Lampin, P. Filloux, C. Manquest, C. Sirtori, I. Sagnes, S. P. Khanna, E. H. Linfield, A. G. Davies, H. Beere, and D. Ritchie, Opt. Express **18,** 20799 (2010).
11. M. Ravaro, P. Gellie, G. Santarelli, C. Manquest, P. Filloux, C. Sirtori, J. F. Lampin, G. Ferrari, S. P. Khanna, E. H. Linfield, H. E. Beere, D. A. Ritchie, and S. Barbieri, IEEE J. Sel. Top. Quant. Electron. **19,** 8501011 (2013).
12. H. C. Liu, C. Y. Song, A. J. S. Thorpe, and J. C. Cao, Appl. Phys. Lett. **84,** 4068 (2011).
13. X. G. Guo, J. C. Cao, R. Zhang, Z. Y. Tan, and H. C. Liu, IEEE J. Sel. Top. Quant. Electron. **19,** 8500508 (2013).
14. P. D. Grant, S. R. Laframboise, R. Dudek, M. Graf, A. Bezinger, and H. C. Liu, Electron. Lett. **45,** 952 (2009).
15. Z. Chen, L. Gu, Z. Tan, C. Wang, and J. Cao, Chin. Opt. Lett. **11,** 112001 (2013).
16. Z. Tan, Z. Chen, J. Cao, and H. Liu, Chin. Opt. Lett. **11,** 031203 (2013).
17. T. Zhou, R. Zhang, X. G. Guo, Z. Y. Tan, Z. Chen, J. C. Cao, and H. C. Liu, IEEE Photon. Technol. Lett. **24,** 1109 (2012).